Spatial and Temporal Electrochemical Control of Singlet Oxygen Production and Decay in Photosensitized Experiments

Vijaykumar S. Ijeri, Kim Daasbjerg, Peter R. Ogilby,* and Lars Poulsen*

Center for Oxygen Microscopy and Imaging, Department of Chemistry, University of Aarhus, Langelandsgade 140, DK-8000 Århus, Denmark

Active spatial and temporal modulation of domains of singlet oxygen activity is demonstrated using electrochemical tools. Using singlet oxygen microscopy in photosensitized experiments, it is shown that singlet oxygen concentrations around an ultramicroelectrode can be controlled by applying a bias voltage to the electrode. Two phenomena that can be exploited separately or collectively are examined: (1) the singlet oxygen concentration can be altered by local oxidation or reduction of the photosensitizer, which is the precursor to singlet oxygen, and (2) the reduction of oxygen to produce the superoxide anion which, among other things, is an effective singlet oxygen quencher, results in a local decrease in the concentration of singlet oxygen around the electrode. Both of these phenomena depend significantly on the diffusion of molecules along concentration gradients established by the biased electrode. The results reported herein demonstrate that one can indeed exert local electrochemical control and readily manipulate the population of singlet oxygen produced in a photosensitized process.

Introduction

The first excited electronic state of molecular oxygen, singlet molecular oxygen, $O_2(a^1\Delta_g)$, is a reactive intermediate that is important in processes ranging from polymer degradation[1] to certain mechanisms of plant defense[2−4] and cell death (e.g., apoptosis).[5] Singlet oxygen is an electrophile with a chemistry unique from that of ground-state oxygen, $O_2(X^3\Sigma_g^-)$, and acts as both an oxidizing as well as oxygenating agent in chemical and biological environments.[6,7] The lifetime of singlet oxygen depends significantly on the solvent, and can range from 3.5 μs in H_2O to 1−50 ms in solvents lacking C−H and O−H bonds.[8] In a given solvent, interactions with other solutes will shorten the lifetime of singlet oxygen by an amount that depends on the interaction rate constant and the concentration of that particular solute. With a finite lifetime, singlet oxygen will thus diffuse over a finite distance from where it was produced. This can have important ramifications under conditions where singlet oxygen is produced in selected domains of a heterogeneous system. Examples of the latter abound in fields ranging from biology to polymer science.

The ability to actively modulate domains of singlet oxygen activity through spatial and temporal control of singlet oxygen production and decay is a topic that has received an increasing amount of attention in recent years.[9] Exerting such control can have a profound impact, particularly in multicomponent systems where the selectivity of singlet-oxygen-dependent processes is important. Moreover, the ability to externally manipulate local

singlet oxygen populations can be a powerful mechanistic tool in the study of many complicated systems. It is this issue of control that we address in the present report.

Although singlet oxygen can be generated in a number of ways, the photosensitized production of singlet oxygen is the approach that is arguably most commonly employed (Figure 1). Molecules (i.e., sensitizers) that absorb light and that efficiently transfer the energy of excitation to ground-state oxygen are abundant. These molecules can be functionalized such as to facilitate preferential solvation in one domain of a phase-separated mixture. Furthermore, light is readily manipulated with spatial, temporal, and spectral degrees of freedom. Thus, the photosensitized process is ideally suited to a study of control in singlet oxygen production. Additionally, and from a more practical perspective, the photosensitized production of singlet oxygen is pertinent to applications that range from the development of electroluminescent devices to photodynamic cancer therapies.[1,10−12]

The superoxide radical anion ($O_2^{\bullet-}$) is the one-electron reduction product of oxygen. In itself, it is a reactive oxygen species that results in lipid peroxidation and protein denaturation, for example.[13] However, when considering mechanisms by which local concentrations of singlet oxygen can be controlled, it is important to recognize that the superoxide anion is an effective quencher of singlet oxygen ($k_q^{SO} = 7 \times 10^9$ M^{-1} s^{-1} in CH_3CN [14]). This quenching occurs through a process of electron transfer as shown in eq 1.[14,15] It is also important to note that the superoxide ion is not consumed in this reaction.

$$O_2^{\bullet-} + {}^1O_2 \xrightarrow{k_q^{SO}} O_2 + O_2^{\bullet-} \qquad (1)$$
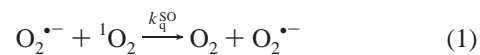
We have recently developed a number of microscopes that allow us to optically create and detect singlet oxygen with both

* Corresponding author. E-mail: progilby@chem.au.dk (P.R.O.); lpoulsen@chem.au.dk (L.P.).
(1) Scurlock, R. D.; Wang, B. J.; Ogilby, P. R.; Sheats, J. R.; Clough, R. L. *J. Am. Chem. Soc.* **1995**, *117*, 10194−10202.
(2) Hideg, E.; Ogawa, K.; Kalai, T.; Hideg, K. *Physiol. Plant.* **2001**, *112*, 10−14.
(3) Chen, W. L.; Xing, D.; Tan, S. C.; Tang, Y. H.; He, Y. H. *Luminescence* **2003**, *18*, 37−41.
(4) Ledford, H. K.; Niyogi, K. K. *Plant Cell Environ.* **2005**, *28*, 1037−1045.
(5) Kochevar, I. E.; Lynch, M. C.; Zhuang, S. G.; Lambert, C. R. *Photochem. Photobiol.* **2000**, *72*, 548−553.
(6) Clennan, E. L.; Pace, A. *Tetrahedron* **2005**, *61*, 6665−6691.
(7) Foote, C. S. *Acc. Chem. Res.* **1968**, *1*, 104−110.
(8) Schweitzer, C.; Schmidt, R. *Chem. Rev.* **2003**, *103*, 1685−1757.
(9) Clo, E.; Snyder, J. W.; Ogilby, P. R.; Gothelf, K. V. *ChemBioChem* **2007**, *8*, 475−481.

(10) Brown, S. B.; Brown, E. A.; Walker, I. *Lancet Oncol.* **2004**, *5*, 497−508.
(11) Dougherty, T. J.; Gomer, C. J.; Henderson, B. W.; Jori, G.; Kessel, D.; Korbelik, M.; Moan, J.; Peng, Q. *J. Natl. Cancer Inst.* **1998**, *90*, 889−905.
(12) Sheats, J. R.; Antoniadis, H.; Hueschen, M.; Leonard, W.; Miller, J.; Moon, R.; Roitman, D.; Stocking, A. *Science* **1996**, *273*, 884−888.
(13) Redmond, R. W.; Kochevar, I. E. *Photochem. Photobiol.* **2006**, *82*, 1178−1186.
(14) Guiraud, H. J.; Foote, C. S. *J. Am. Chem. Soc.* **1976**, *98*, 1984−1986.
(15) Mulazzani, Q. G.; Dangelantonio, M.; Venturi, M.; Rodgers, M. A. J. *J. Phys. Chem.* **1991**, *95*, 9605−9608.
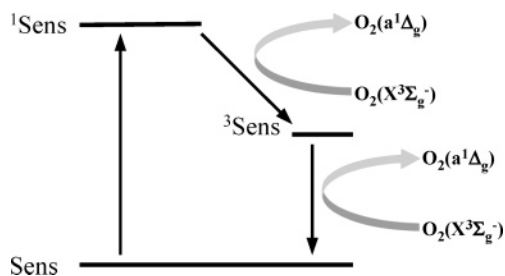
Figure 1. Scheme illustrating the photosensitized production of singlet oxygen. For most molecules used as sensitizers, the sensitizer triplet state is the immediate precursor to singlet oxygen. However, some molecules have a singlet excited-state with a sufficiently long lifetime and a singlet–triplet energy gap that is sufficiently large that singlet oxygen can also be produced in the process of oxygen-induced intersystem crossing.

spatial and temporal resolution.[16] We have shown that these microscopes can be used to study the behavior of singlet oxygen in heterogeneous systems that range from single biological cells to phase-separated polymers.[16] These optical tools constitute an important component in a program to exert control over singlet oxygen production. For the present study, we set out to explore how electrochemical tools could likewise be used to control both the production and decay of singlet oxygen in spatially and temporally resolved experiments. The approach involves the use of ultramicroelectrodes to (1) switch electrochemically active photosensitizers off and on and (2) generate the superoxide ion which, among other things, will deactivate singlet oxygen.

Experimental Section

Chemicals. Perinaphthenone (PN), which is also commonly called 1-phenalenone, was used as received (97%, Aldrich). Perylene (99%, Aldrich), 5,10,15,20-tetraphenylporphyrin zinc(II), (Zn–TPP, Aldrich), and acetonitrile (anhydrous, 99.9%, Lab-Scan) were likewise used as received. The water content in the acetonitrile after exposure to the air in the laboratory was determined using Karl Fischer titration. Tetrabutylammonium hexafluorophosphate (Bu$_4$NPF$_6$) was prepared using standard procedures.[17] Pyrene-1,6-dione (PD) was synthesized using the approach of Fatiadi.[18,19]

Microscopes. Spatially resolved singlet oxygen phosphorescence experiments were performed using a modified Olympus inverted microscope (model IX70) equipped with infrared optics and a cooled InGaAs linear array detector (custom-modified OMA V, Roper/ Princeton Instruments) in an approach that has been described previously.[16,20] Images based on the sample fluorescence in the visible region of the spectrum were recorded on the same microscope using an Evolution QEi fluorescence camera (MediaCybernetics). In these experiments, the excitation source was the output of a 75 W Xe lamp that had been passed through a water filter, heat mirror (CVI, Inc.), a series of KG heat-absorbing filters (Schott), and a 425 nm band-pass filter (40 nm full width at half-maximum (fwhm), Chroma Technology) before being reflected onto the sample by a dichroic mirror (780DCXRU, Chroma Technologies). The excitation power in the focus of the microscope was 0.1–0.3 W cm^{-2}. Singlet oxygen phosphorescence was spectrally isolated using a 1270 nm band-pass filter (50 nm fwhm, Barr Associates), whereas sample fluorescence was spectrally isolated using a 535 nm band-pass filter (40 nm fwhm, Chroma Technology). Laser scanning singlet oxygen microscopy

was performed in a photon-counting experiment on a different microscope (a modified Olympus model IX71) using a cooled near-infrared photomultiplier tube (Hamamatsu model R5509–42) and 400 nm laser excitation as previously described.[21] Unless otherwise stated, typical acquisition times for both microscopes were 30–180 s.

Singlet Oxygen Quantum Yields. The quantum yield of singlet oxygen production from Zn–TPP was determined in a time-resolved experiment in which the sensitizer was irradiated using the 355 nm third harmonic of a nanosecond Nd:YAG laser (Quanta Ray GCR 230). The 1270 nm singlet oxygen phosphorescence was monitored through a band-pass filter (50 nm fwhm, Barr Associates) using a cooled Ge detector (North Coast model EO-817P). Values for the phosphorescence intensity were obtained by extrapolating the time-resolved signal to zero time, and recording such data over a wide range of incident laser powers.[22] Corresponding data were recorded from PN, which was used as a reference standard. Experiments were performed in air-saturated solutions.

Electrochemical Apparatus. A 4 cm × 1 cm quartz cuvette (Hellma) with a transparent optical quality base window and a lid modified to hold electrodes was used as an electrochemical cell. This cell was placed on the stage of the inverted microscope, and all optical experiments were performed through the base window. Working electrodes of either platinum or glassy carbon were used. In the first case, a platinum wire (250 μm diameter, Aldrich) was sealed into a Teflon tube using an epoxy glue and, at one end of the tube, ~5 mm of the wire was exposed to the solution. In the other cases, glass-encased 33 and 7 μm diameter glassy carbon disc ultramicroelectrodes or a Teflon-encased 3 mm diameter glassy carbon disc electrode was used. These latter electrodes were obtained from CH Instruments. A silver wire immersed in a glass tube containing the supporting electrolyte, separated from the main solution by a porous glass frit, was used as the quasi reference electrode, and a platinum wire served as the counter electrode. After every set of experiments, the potential of the ferrocenium/ferrocene couple (Fc$^+$/ Fc) was measured with the respective working electrode, and all potentials are reported with reference to Fc$^+$/Fc.[23] The potential of Fc$^+$/Fc has been measured to 0.41 V versus a saturated calomel electrode.[24] The CHI 660B potentiostat from CH Instruments was used for all electrochemical measurements. All experiments were done at ambient temperature in air-saturated acetonitrile (~1.8 mM oxygen), unless otherwise stated. In steady-state experiments, measurements of the singlet oxygen phosphorescence intensity were performed after the electrode current had stabilized (5–10 s depending on the electrode).

Simulations. To complement the combined optical and electrochemical experiments performed using disc ultramicroelectrodes, the concentration profiles of oxygen, superoxide, and singlet oxygen were modeled by means of numerical simulations based on the finite element method performed using the COMSOL Multiphysics package (version 3.3, COMSOL, Sweden).

Results and Discussion

Electrochemical Modulation of the ^{1}O$_2$ Phosphorescence Signal. Initial experiments were performed in acetonitrile using PN as a singlet oxygen sensitizer and a focused laser to produce singlet oxygen in close proximity to an electrode surface. PN has a quantum efficiency of singlet oxygen production near unity in acetonitrile ($\Phi_\Delta = 0.98 \pm 0.05$) and is commonly used as a standard for quantitative singlet oxygen studies.[19,25] The ir-radiating laser beam was focused just below a 3 mm diameter

(16) Snyder, J. W.; Zebger, I.; Gao, Z.; Poulsen, L.; Frederiksen, P. K.; Skovsen, E.; McIlroy, S. P.; Klinger, M.; Andersen, L. K.; Ogilby, P. R. *Acc. Chem. Res.* **2004**, *37*, 894–901.

(17) Sawyer, D. T.; Sobkowiak, A.; Roberts, J. L., Jr. *Electrochemistry for Chemists*, 2nd ed.; John Wiley & Sons: New York, 1995.

(18) Fatiadi, A. J. *J. Chromatog.* **1965**, *20*, 319.

(19) Arnbjerg, J.; Paterson, M. J.; Nielsen, C. B.; Jørgensen, M.; Christiansen, O.; Ogilby, P. R. *J. Phys. Chem. A* **2007**, *111*, 5756–5767.

(20) Zebger, I.; Poulsen, L.; Gao, Z.; Andersen, L. K.; Ogilby, P. R. *Langmuir* **2003**, *19*, 8927–8933.

(21) Skovsen, E.; Snyder, J. W.; Lambert, J. D. C.; Ogilby, P. R. *J. Phys. Chem. B* **2005**, *109*, 8570–8573.

(22) Scurlock, R. D.; Nonell, S.; Braslavsky, S. E.; Ogilby, P. R. *J. Phys. Chem.* **1995**, *99*, 3521–3526.

(23) Singh, P. S.; Evans, D. H. *J. Phys. Chem. B* **2006**, *110*, 637–644.

(24) Daasbjerg, K.; Pedersen, S. U.; Lund, H. In *General Aspects of the Chmistry of Radicals*; Alfassi, Z. B., Ed.; John Wiley & Sons: Chichester, U.K., 1999; p 385.

(25) Schmidt, R.; Tanielian, C.; Dunsbach, R.; Wolff, C. *J. Photochem. Photobiol. A* **1994**, *79*, 11–17.

Table 1. Photochemical and Electrochemical Properties of Pertinent Molecules

molecule	Φ_Δ in air-saturated CH_3CN	first redox peak $(E_p/V)^a$
oxygen		$E_{pc} = -1.48^b$ and -1.98^c
PN	0.98 ± 0.05^d	$E_{pc} = -1.57^b$
perylene		$E_{pc} = -2.17^b$
PD	1.0 ± 0.05^d	$E_{pc} = -0.89^c$
Zn—TPP	0.82 ± 0.05	$E_{pa} = 0.42^c$

[a] In CH_3CN vs Fc^+/Fc. E_{pc} and E_{pa} are the cathodic (i.e., reduction) and anodic (i.e., oxidation) peak potentials, respectively. [b] At glassy carbon electrode. [c] At Pt wire electrode. [d] From Arnbjerg et al.[19]

glassy carbon electrode, and the singlet oxygen phosphorescence intensity emanating from the small volume defined by the laser spot was monitored as a function of the potential applied to the electrode. Although the reduction potential of PN is quite close to that of oxygen (Table 1, Figure 2), the cyclic voltammogram of an air-saturated solution of acetonitrile containing a small amount of PN (50 μM) principally resembles that of oxygen because of the high concentration of the latter ($\sim$1.8 mM) (Figure 2a,b). The voltage-dependent intensity of the singlet oxygen phosphorescence signal, measured as photon counts, is overlaid on the cyclic voltammogram of PN in aerated acetonitrile (Figure 2a).

The data in Figure 2a indicate that the singlet oxygen phosphorescence intensity is constant until a potential of about -1.1 V is applied. Thereafter, as the potential is made more negative, the singlet oxygen signal intensity decreases and reaches the background value at a potential near -1.30 V. The removal of the singlet oxygen signal upon sudden application of -1.50 V to the electrode was found to take approximately 1 min, and, similarly, the signal was recovered 1 min after turning the potential off (Figure 2c). This decrease in singlet oxygen phosphorescence intensity at negative potentials could originate from at least three different phenomena acting simultaneously or independently: (i) electrochemical reduction of the sensitizer, which could adversely influence singlet oxygen production; (ii) a decrease in the concentration of ground-state oxygen around the electrode due to electrochemical reduction (i.e., $O_2(X^3\Sigma_g^-) + e^- \rightarrow O_2^{\bullet-}$) which, in turn, would result in a smaller fraction of sensitizer triplet states that are quenched by $O_2(X^3\Sigma_g^-)$ to produce singlet oxygen; and (iii) quenching of singlet oxygen by the superoxide ion formed through the reduction of oxygen. With these points in mind, we set out to investigate these phenomena separately.

Prior to discussing these independent studies, however, it is important to address one subtle point with respect to the data shown in Figure 2. As an excited state of oxygen, singlet oxygen should be reduced to superoxide more easily than ground-state oxygen. Given that the excitation energy of singlet oxygen is $\sim$0.98 eV[8] and that the onset of ground-state oxygen reduction occurs at approximately -1.1 V in acetonitrile (*vide supra*), reduction of singlet oxygen is expected at approximately -0.1 V. Thus, in principle, singlet oxygen phosphorescence intensities recorded at electrode potentials more negative than -0.1 V should be smaller than those recorded at electrode potentials more positive than -0.1 V. The data in Figure 2 clearly show that this is not the case. The most likely explanation for this observation is that, despite a focused excitation volume adjacent to the electrode, only a small fraction of the singlet oxygen produced in this volume is close enough to the electrode to be reduced (i.e., this particular electrode-dependent change in our optical signal is too small to be resolved). Note also that any superoxide formed at the electrode surface upon the reduction of singlet oxygen will be immediately oxidized to ground-state oxygen at potentials more positive than approximately -1.1 V. Thus, at electrode

potentials between -1.1 and -0.1 V, no net current will flow, and the electrode surface will simply act as a singlet oxygen quencher.

Electrochemical Modulation of Sensitizer Properties. To investigate the effect of changes in the oxidation state of the singlet oxygen photosensitizer, a series of combined electrochemical/optical experiments was performed under conditions where oxygen is not directly reduced at the electrode. Thus, in this study, we attempt to preclude any effect that oxygen depletion and/or superoxide creation might have on our optical signal. The photochemical and electrochemical properties of the sensitizers used for this study are summarized in Table 1. Two different sensitizers were examined: one that is readily reduced (PD) and another that is readily oxidized (Zn—TPP). In these experiments, line-scan images based on singlet oxygen phosphorescence were used, yielding information about the spatial profile of singlet oxygen around the electrode which, in this case, was a 250 μm diameter platinum wire. Singlet oxygen has a lifetime τ_Δ of $\sim$80 μs in acetonitrile,[26] and thus the mean radial diffusion length l_r is expected to be $\sim$1.8 μm over this period of time [i.e., $l_r = (6D_O\tau_\Delta)^{1/2}$, where a diffusion coefficient, D_O, for oxygen of 7.1 $\times 10^{-5}$ cm^2 s^{-1} in acetonitrile[27] was used].

Effect of Sensitizer Reduction. PD has a singlet oxygen quantum yield of unity in acetonitrile.[19] Also, PD does not luminesce and, as such, will not interfere with a singlet oxygen phosphorescence experiment. PD undergoes a two-step reduction (Figure 3b). The first reduction at -0.89 V is reversible and is unaffected by the presence or absence of oxygen in solution. At this potential, no reduction of oxygen takes place at the Pt wire electrode (*vide supra*, Figure 2). The second reduction peak at -1.3 V is less well-defined, and, in the presence of oxygen, the peak is obscured as the reduction of oxygen starts around this potential.

Using the imaging singlet oxygen microscope, the singlet oxygen phosphorescence signal in a line across the wire electrode was monitored at different potentials (Figure 3a). The geometry of the optical experiment is such that the array detector of the microscope looks up through the solution toward the bottom of the cylindrical electrode (i.e., the long axis of the electrode is positioned perpendicular to the image plane of the microscope). Because of the relatively large depth of field inherent to this method and since no singlet oxygen can be produced in the volume taken up by electrode, the electrode itself appears as a depression in the line-scan of singlet oxygen phosphorescence intensity (see Figure 3a). At open circuit (no potential applied) or -0.36 V, where no electrochemical reaction takes place, an intense singlet oxygen phosphorescence signal is seen all around the electrode. At an electrode potential of -0.96 V, which is more negative than the first reduction peak of PD, we observe a decrease in the intensity of singlet oxygen phosphorescence around the electrode. At electrode potentials of -1.26 V, near the second reduction peak of PD, and at -2.06 V, where oxygen is reduced to superoxide, successively greater decreases in the intensity of the singlet oxygen signal are observed.

It is apparent from the data in Figure 3a that the change in singlet oxygen phosphorescence intensity does not occur uniformly as a function of the distance from the electrode. Rather, the intensity profile indicates a nonuniform distribution of singlet oxygen around the electrode. These data reflect effects of the electrode geometry (i.e., edges and unevenness of the electrode surface), which are common when one uses a comparatively large wire for this purpose. More uniform behavior is observed when using smaller disk electrodes (*vide infra*).

(26) Scurlock, R. D.; Ogilby, P. R. *J. Photochem. Photobiol. A* **1993**, *72*, 1−7.
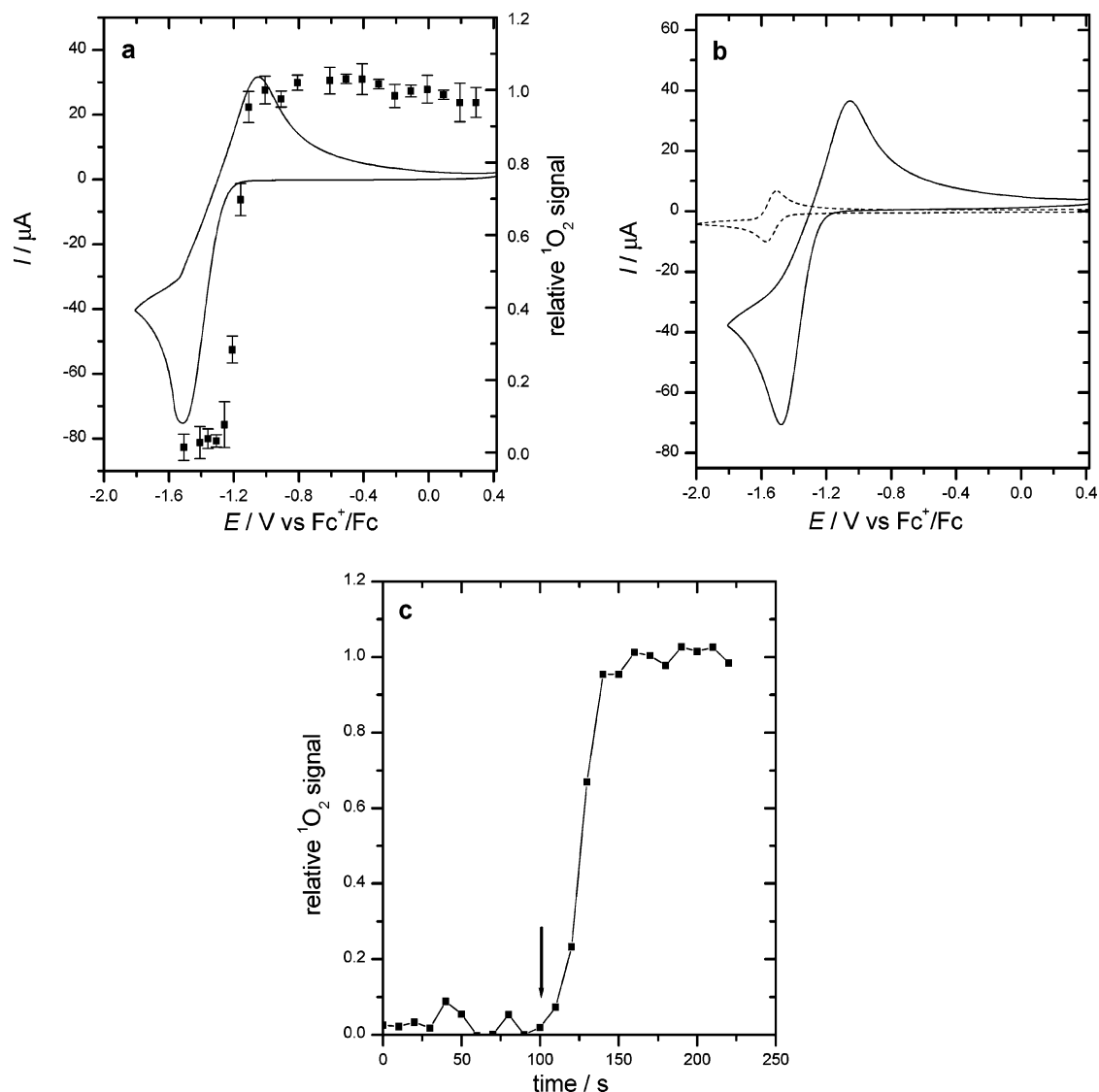(27) Tsushima, M.; Tokuda, K.; Ohsaka, T. *Anal. Chem.* **1994**, *66*, 4551−4556.

Figure 2. (a) Cyclic voltammogram recorded from air-saturated acetonitrile containing 50 μM PN (left axis). The data were recorded using a 3 mm diameter glassy carbon electrode at a sweep rate of 0.1 V s^{-1}. Also shown is the voltage-dependent intensity of the singlet oxygen phosphorescence signal recorded upon 400 nm irradiation with a laser focused just below the electrode (right axis). (b) Cyclic voltammograms of 0.22 mM PN in deoxygenated acetonitrile (dashed line) and of oxygen in air-saturated acetonitrile (solid line) at a sweep rate of 0.1 V s^{-1}. All solutions contain 0.05 M Bu$_4$NPF$_6$. (c) Recovery of the singlet oxygen phosphorescence signal after the electrode potential (-1.5 V) was turned off. Arrow indicates the point at which the potential was removed.

The data in Figure 3a clearly indicate that reduction of PD adversely affects the steady-state concentration of singlet oxygen around the electrode. One possible explanation for these data is that, upon reduction, the PD radical anion diffuses away from the electrode, whereupon, taking into account that the reduction potential of O$_2$(a¹Δg) is estimated to be approximately -0.1 V (*vide supra*), it can transfer an electron to singlet oxygen (i.e., PD$^{\bullet-}$ + O$_2$(a¹Δg) → PD + O$_2^{\bullet-}$). In turn, the superoxide thus formed in this process could quench singlet oxygen. Alternatively, the data may simply imply that, upon reduction, PD becomes a less efficient singlet oxygen photosensitizer upon irradiation at 425 nm. The mechanistic details for a decrease in the yield of singlet oxygen in this case could reflect a number of different phenomena (e.g., changes in sensitizer absorption spectrum, the creation of different excited states with lifetimes that preclude singlet oxygen production, a decrease in the efficiency of energy transfer to ground-state oxygen, etc.).

In support of the reasonable expectation that the excited states of PD$^{\bullet-}$ exhibit different behavior compared to those of PD, we observed a green fluorescence (emission maximum at 500 nm)

around the electrode immersed in a solution of PD whenever the potential was more negative than approximately -0.70 V. This observation was further investigated using a 33 μm glassy carbon disc ultramicroelectrode and a wide-field fluorescence microscope. Fluorescence was again recorded looking up through the solution at the electrode, and images were obtained as a function of the applied potential (Figure 4). This green fluorescence was also observed in deoxygenated solutions ruling out possible interactions between the radical anion and oxygen as the cause of the fluorescence. These data indicate that PD$^{\bullet-}$ or an oxygen-independent derivative of PD$^{\bullet-}$ has a highly fluorescent state. This observation and interpretation are consistent with those made in related experiments on similar aromatic ketones such as benzo[a]pyrenediones.[28] The radical anions of these latter compounds are known to form ketyl radicals by proton abstraction from residual water in the solvent, and these radicals have unique absorption and emission spectra.[29] The observation of intense

(28) Liao, K. H.; Mayeno, A. N.; Reardon, K. F.; Yang, R. S. H. *J. Chromatogr. B* **2005**, *824*, 166–174.
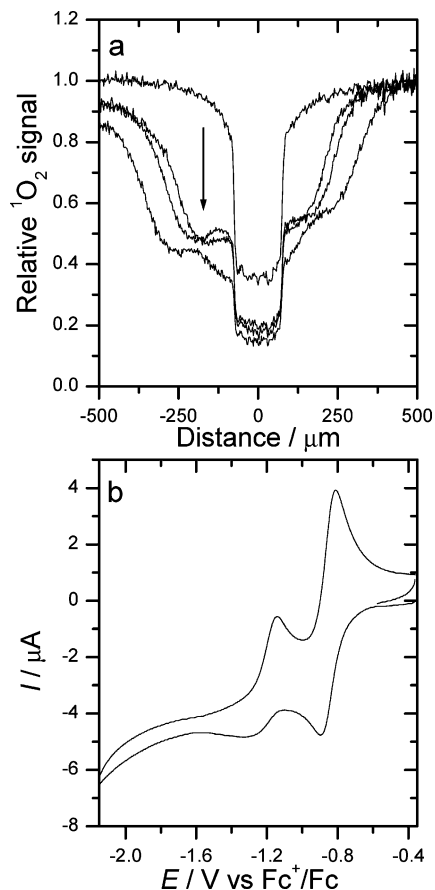
Figure 3. (a) Effect of sensitizer reduction on the spatial profile of singlet oxygen concentration around a 250 μm diameter Pt wire electrode. The sensitizer used was PD (0.19 mM). Data obtained from the InGaAs linear array detector show the intensity of singlet oxygen phosphorescence plotted against the spatial coordinate for four different potentials applied to the electrode: -0.36, -0.96, -1.26, and -2.06 V. The arrow indicates the direction of increasingly negative potentials. The electrode itself is seen as a depression in the singlet oxygen signal (the center of the electrode is used to establish the origin of the distance scale). (b) Cyclic voltammogram recorded from deoxygenated acetonitrile containing 0.19 mM PD and 0.05 M Bu$_4$NPF$_6$ using the same 250 μm diameter Pt wire electrode at a sweep rate of 0.1 V s^{-1}.

fluorescence from the reduced form of PD also requires a corresponding decrease in the PD$^{\bullet-}$-sensitized yield of singlet oxygen.

Effect of Sensitizer Oxidation. Having shown that reduction of the photosensitizer can decrease the concentration of singlet oxygen surrounding the electrode, as manifested in the intensity of the singlet oxygen phosphorescence, we set out to investigate whether a similar effect could be observed by oxidizing the sensitizer. For this purpose, Zn–TPP was chosen as the singlet oxygen sensitizer. Zn–TPP not only produces singlet oxygen in appreciable yield in acetonitrile, but it also has two well-defined and reversible oxidation peaks: the first at 0.42 V and the second at 0.77 V (Figure 5b). These experiments were performed upon irradiation of the sample through a 425 nm band-pass filter with 40 nm fwhm, which is spectrally coincident with the Soret absorption band of Zn–TPP.

At an applied potential of -0.33 V, the Zn–TPP-sensitized singlet oxygen phosphorescence intensity around the electrode was the same as that without any bias on the electrode. However,
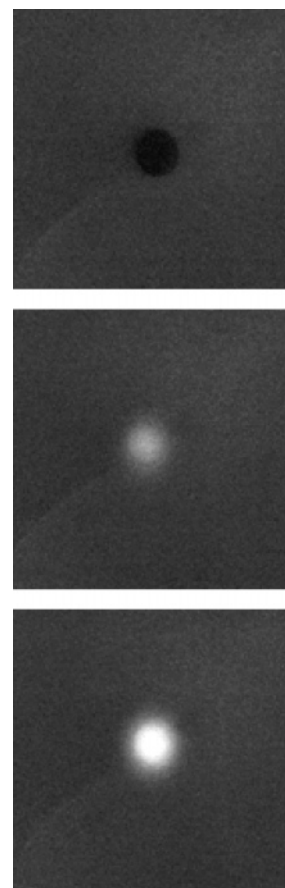

Figure 4. Fluorescence recorded around a 33 μm carbon disc ultramicroelectrode immersed in an acetonitrile solution of PD (97 μM). The data were recorded through a 535 nm band-pass filter (40 nm fwhm). Images were obtained at electrode potentials of -0.6 (top), -0.9 (middle), and -1.0 V (bottom). At potentials more positive than approximately -0.7 V, one simply observes the shadow of the electrode in the fluorescence image (top panel). As the potential is made more negative than approximately -0.7 V, which corresponds to the onset of the reduction of PD (see Figure 3b), a green fluorescence is observed from the solution surrounding the electrode.

upon increasing the potential to 0.42 V, at which point one-electron oxidation of Zn–TPP occurs, a decrease in the intensity of the singlet oxygen signal around the electrode was seen. A further decrease in signal intensity was observed when the applied potential was increased to 0.77 V, which corresponds to the second oxidation peak of Zn–TPP. The data are shown in Figure 5a.

When Zn–TPP is oxidized to the corresponding radical cation, the molecule's main absorption band (i.e., the Soret band) is perturbed, and its extinction coefficient at 425 nm decreases relative to that of the parent compound.[30] It has also been shown that the major deactivation pathway for the excited-state radical cation is fast internal conversion from the lowest excited doublet state to the doublet ground state.[30] With these points in mind, it is reasonable to conclude that our potential-dependent Zn–TPP data reflect a change in the efficiency with which singlet oxygen is produced upon irradiation at 425 nm.

In these experiments with sensitizer reduction and oxidation, it is important to note that the respective processes are all reversible. As such, in a given experiment, when the electrode potential was returned to a potential where the redox process is

(29) Okutsu, T.; Noda, S.; Tanaka, S.; Kawai, A.; Obi, K.; Hiratsuka, H. *J. Photochem. Photobiol. A* **2000**, *132*, 37–41.

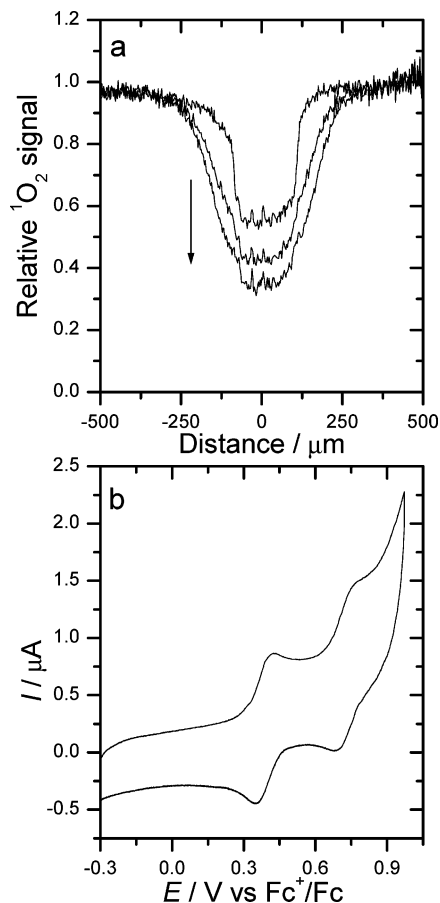(30) Okhrimenko, A. N.; Gusev, A. V.; Rodgers, M. A. J. *J. Phys Chem. A* **2005**, *109*, 7653–7656.

Figure 5. (a) Effect of sensitizer oxidation on the spatial profile of singlet oxygen concentration around a 250 μm diameter Pt electrode. The sensitizer used was Zn−TPP (40 μM). Data obtained from the InGaAs linear array detector show the intensity of singlet oxygen phosphorescence plotted against the spatial coordinate for three different potentials applied to the electrode: −0.33, 0.42, and 0.77 V. The arrow indicates the direction of increasingly positive potentials. The electrode itself is seen as a depression in the singlet oxygen signal (the center of the electrode is used to establish the origin of the distance scale). (b) Cyclic voltammogram recorded from air-saturated acetonitrile containing 40 μM Zn−TPP and 0.05 M Bu₄NPF₆ using the same 250 μm diameter Pt wire electrode at a sweep rate of 0.1 V s⁻¹.

reversed, we were able to recover the original intensity of the singlet oxygen phosphorescence signal.

Effect of Oxygen Reduction. Having shown that we can reversibly modulate the concentration of singlet oxygen near an electrode by reducing or oxidizing the sensitizer, we set out to explore the effects of selectively reducing oxygen at the electrode. The expectation in this case is that, upon the reduction of oxygen to produce the superoxide ion, at least three things could occur to decrease the intensity of the singlet oxygen phosphorescence signal around the electrode. The first is that, through this reduction, we would deplete the local concentration of ground-state oxygen which, depending on the sensitizer, could result in a smaller fraction of sensitizer excited states that are quenched to produce singlet oxygen. Second, the superoxide ion could deactivate the sensitizer triplet state,[31] which, in turn, would likewise influence the amount of singlet oxygen produced. Finally, the superoxide ion formed could deactivate a significant fraction of the singlet oxygen present. Superoxide is an efficient quencher of singlet oxygen in acetonitrile.[14,15]

With this experiment in mind, the molecule perylene was chosen as the singlet oxygen sensitizer. From the electrochemical perspective, perylene is an ideal choice in that it has a reduction potential that is significantly more negative than that of oxygen (Figure 6). Thus, it is possible to selectively reduce oxygen to superoxide without changing the oxidation state of perylene. From the photophysics perspective, the excited-state behavior of perylene depends significantly on the ambient oxygen concentration. Specifically, in the absence of oxygen, perylene has a very low yield of intersystem crossing to produce the triplet state.[32] As the ambient oxygen concentration is increased, however, quenching of the sensitizer singlet state by oxygen induces intersystem crossing, which, in turn, is manifested in increased yields of singlet oxygen [i.e., the singlet−triplet energy gap in perylene is sufficiently large that oxygen-induced intersystem crossing can result in the production of singlet oxygen (Figure 1), and the triplet state thus produced can also sensitize the production of singlet oxygen]. Thus, the perylene-sensitized production of singlet oxygen depends greatly on the ambient oxygen concentration.[32−34]

As seen in Figure 6, irradiation of an air-saturated solution of perylene in acetonitrile gives rise to a population of singlet oxygen that is readily monitored using our spatially resolved detector. It is important to note that, under these conditions, only a small fraction of the perylene singlet state is being quenched by oxygen, and the quantum yield of singlet oxygen production is only ∼0.07.[32] Upon applying −1.85 V to the electrode, which is sufficient to reduce oxygen to superoxide without changing the oxidation state of perylene, we clearly see a decrease in the singlet oxygen intensity surrounding our electrode.

In these experiments, 33 and 7 μm diameter glassy carbon disc ultramicroelectrodes were used. A characteristic of these disc electrodes is that the sides of the electrode are covered with a several-millimeters-thick glass coating, and only the bottom of the electrode is exposed to the solution, yielding a small and uniform surface. Because of the glass coating, the "shadow" of the entire electrode assembly in our near-IR image is much larger than the field of view and does not contribute to the shape of the line-scan profile. In comparison to the platinum electrodes used in our other experiments (*vide supra*), the use of these smaller glassy carbon electrodes also has the advantages that (1) oxygen reduction occurs at a less negative potential at this material,[35] and (2) we create a homogeneous spatial distribution of reduced species around the electrode.

Using this perylene-sensitized system, one can nicely illustrate the concept of temporal and spatial control of the singlet oxygen concentration in a number of ways (Figure 7). First, by putting an increasingly more negative potential on the electrode, the local concentration of singlet oxygen can be decreased (up to the point that the production of superoxide is limited by the diffusion of oxygen to the electrode). Furthermore, when the potentials are switched back and forth between values where oxygen reduction or superoxide oxidation takes place, a simultaneous change in the singlet oxygen phosphorescence signal around the electrode is observed, demonstrating the "switchability" of the singlet oxygen concentration in a localized domain. Finally, one can also move the electrode to a different position in the sample and selectively decrease the local concentration of singlet oxygen in a chosen spatial domain.

(31) Hoytink, G. J. *Acc. Chem. Res.* **1969**, *2*, 114−120.

(32) Abdel-Shafi, A. A.; Worrall, D. R. *J. Photochem. Photobiol. A* **2005**, *172*, 170−179.

(33) Iu, K. K.; Ogilby, P. R. *J. Phys. Chem.* **1988**, *92*, 4662−4666.

(34) Kristiansen, M.; Scurlock, R. D.; Iu, K. K.; Ogilby, P. R. *J. Phys. Chem.* **1991**, *95*, 5190−5197.

(35) Sawyer, D. T.; Chlericato, G.; Angelis, C. T.; Nanni, E. J.; Tsuchiya, T. *Anal. Chem.* **1982**, *54*, 1720−1724.
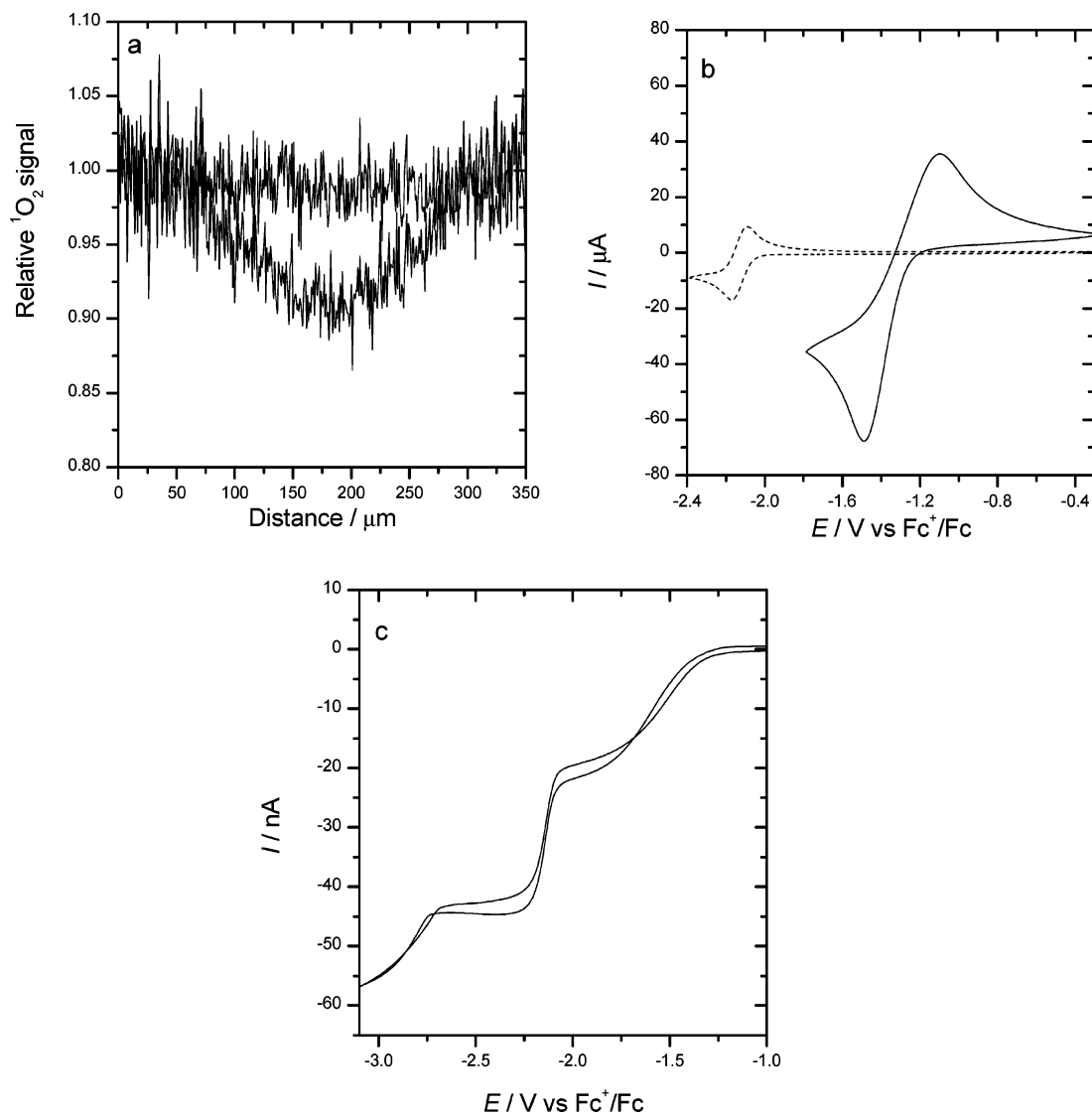
Figure 6. (a) The change in the singlet oxygen phosphorescence intensity around an ultramicroelectrode upon the electrochemical production of the superoxide ion. Two line scans of the singlet oxygen signal across a 7 μm glassy carbon disc ultramicroelectrode are shown: one recorded at an electrode potential of -0.35 V and another at a potential of -1.85 V. At these potentials, the sensitizer, perylene, is not reduced. However, at potentials more negative than -1.35 V, oxygen is reduced to superoxide, which, among other things, can quench singlet oxygen. The perylene concentration was 0.15 mM. (b) Cyclic voltammograms of oxygen (solid line) and 0.8 mM perylene (dashed line) in acetonitrile recorded using a 3 mm glassy carbon disc electrode at a sweep rate of 0.1 V s^{-1}. (c) Steady-state cyclic voltammogram showing the stepwise reduction of oxygen and perylene at a 33 μm diameter glassy carbon disc ultramicroelectrode in acetonitrile (partially deoxygenated solution) at a sweep rate of 0.01 V s^{-1}. All solutions contain 0.05 M Bu$_4$NPF$_6$.

Simulating the Effects of Oxygen Reduction. To help elucidate the molecular events in the experiments described above, we set out to numerically simulate the effects of oxygen reduction on the spatially resolved intensity of the perylene-sensitized singlet oxygen signal. In this simulation, we only considered the following aspects of the problem: (1) the decrease in the ground-state oxygen concentration around the electrode due to the electrochemical reduction that produces the superoxide ion, as well as the associated decrease in the yield of sensitized singlet oxygen production, and (2) the diffusion of the superoxide ion away from the electrode and the resultant quenching of singlet oxygen by superoxide in this spatial domain. The pertinent parameters used to model these phenomena are given in Table 2.

The combined electrochemical/optical experiment was simulated in a two-dimensional (2D) model using steady-state conditions with rotational symmetry around the center of the disc electrode (see Figure 8). Because of the long lifetime and, consequently, long diffusion length of the superoxide radical

anion, a model with large dimensions was used (i.e., a radius around and depth below the electrode of 1 cm was used). Steady-state production of superoxide at the electrode surface was assumed (see Figure 6c), and the opposing fluxes of superoxide and oxygen at the electrode surface were estimated from the experimentally measured current. The remaining nonelectrode part of the top boundary was made impermeable to all species corresponding to the experimental conditions where the boundary consisted of the thick glass coating on the sides of the carbon element. At a distance of 1 cm below and to the side of the electrode, the oxygen concentration was kept constant to mimic equilibrium with the surrounding atmosphere. At the same time, the singlet oxygen and superoxide concentrations were kept at zero at these boundaries. Singlet oxygen was assumed to be produced uniformly and at a rate of $R_{ex}\Phi_\Delta$, where R_{ex} is the rate of light absorption and Φ_Δ is the singlet oxygen quantum yield. R_{ex} was estimated from the size of the illuminated area, the light flux in the microscope, and the absorbance of the sensitizer.
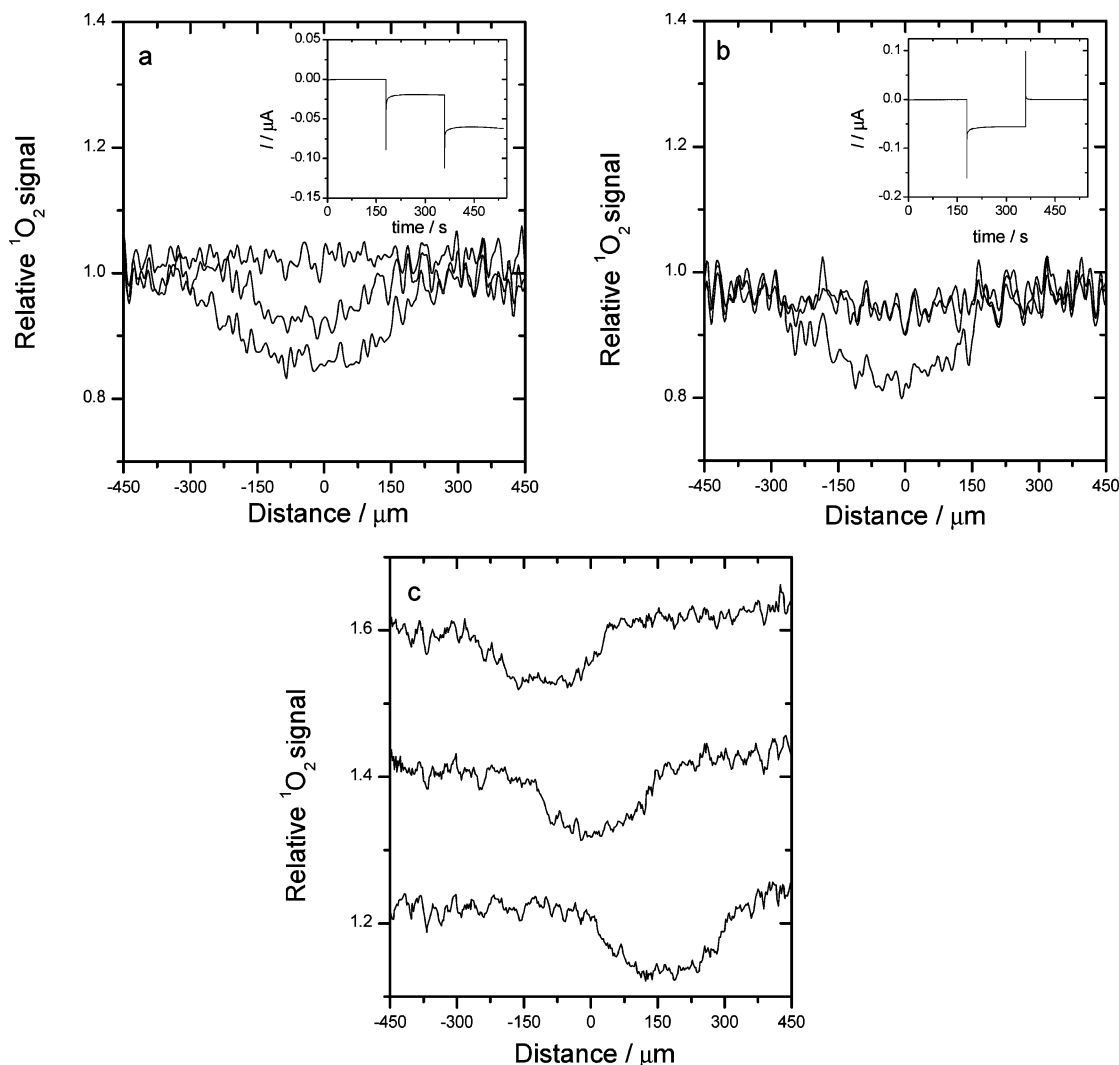
Figure 7. (a,b) Data showing the control of the singlet oxygen concentration around a disc ultramicroelectrode using different potentials. The electrode current measured at each potential is shown in the insert. Data were recorded using a 33 μm glassy carbon disc ultramicroelectrode and 0.13 mM perylene in 0.05 M Bu₄NPF₆/acetonitrile. In panel a we show that, as the electrode potential is stepped to more negative values (−0.85 V, −1.55 V, −1.85 V), superoxide production increases, and the singlet oxygen concentration is lowered. In panel b we show that, when the potentials are switched back and forth between values where oxygen reduction or superoxide oxidation takes place (−1.85 V and −0.85 V, respectively), a corresponding change in the singlet oxygen phosphorescence signal around the electrode is observed. (c) The spatial domain of singlet oxygen depletion changes as the electrode is moved relative to the detector array. For these data, recorded using 0.79 mM PN and a 15 μm Pt disc ultramicroelectrode, we have displaced the respective singlet oxygen scans along the vertical axis to better illustrate this phenomenon.

Superoxide is stable in acetonitrile, and the reduction of oxygen is thus chemically reversible and electrochemically quasi-reversible (Figure 2).[23] Nevertheless, superoxide's lifetime is limited by traces of water in the acetonitrile. In the presence of water, superoxide is protonated to yield the hydroperoxyl radical (O₂•⁻ + H₂O → HO₂• + OH⁻) which, in turn, may oxidize an additional superoxide radical anion to oxygen (HO₂• + O₂•⁻ → HO₂⁻ + O₂).[23,36] The kinetics of this water-induced disproportionation in acetonitrile has been studied by Che et al.[36] On the basis of their data, which indicate that, under the present conditions, protonation of superoxide is the rate-limiting step leading to single exponential behavior for the first 80% of the decay of superoxide, we approximate the disproportionation of superoxide as a pseudo-first-order process with respect to superoxide. In our experiments, the initially anhydrous acetonitrile was allowed to equilibrate with the ambient atmosphere. Although the actual water content in a given sample depended on the

ambient humidity at the time of the experiment, typical water concentrations were measured to be on the order of 0.1 M, which corresponds to a superoxide lifetime of ∼2000 s. As a result, superoxide can diffuse several millimeters within its lifetime, resulting in a concentration gradient around the electrode that is easily resolved with our microscope. In contrast, the shorter-lived singlet oxygen has a mean diffusion length of less than 2 μm in acetonitrile (*vide supra*).

In the simulations, the concentrations of the three oxygen-derived species were described by the following diffusion equations:

$$\frac{\partial[O_2]}{\partial t} - D_O \nabla^2[O_2] = -R_{ex}\Phi_\Delta + k_d^{SO}[O_2^{\bullet-}] + k_d^\Delta[^1O_2] + k_q^{SO}[O_2^{\bullet-}][^1O_2]$$

$$\frac{\partial[^1O_2]}{\partial t} - D_\Delta \nabla^2[^1O_2] = R_{ex}\Phi_\Delta - k_d^\Delta[^1O_2] - k_q^{SO}[O_2^{\bullet-}][^1O_2]$$

(36) Che, Y.; Tsushima, M.; Matsumoto, F.; Okajima, T.; Tokuda, K.; Ohsaka, T. *J. Phys. Chem.* **1996**, *100*, 20134−20137.

$$\frac{\partial[O_2^{\bullet-}]}{\partial t} - D_{SO}\nabla^2[O_2^{\bullet-}] = -2k_d^{SO}[O_2^{\bullet-}] \qquad (2)$$

In eq 2, k_d^{SO} and k_d^{Δ} are the rate constants for the decay of superoxide and singlet oxygen, respectively, in acetonitrile, and k_q^{SO} is the quenching rate constant of singlet oxygen by superoxide. The respective diffusion coefficients are denoted by D. Note that the diffusion coefficient of superoxide, D_{SO}, is smaller than that of ground-state oxygen, D_O, because of stronger solvation by acetonitrile.[37] We have also assumed that the diffusion coefficient for singlet oxygen, D_{Δ}, is the same as that for ground-state oxygen, D_O, despite the fact that the polarizabilities of the
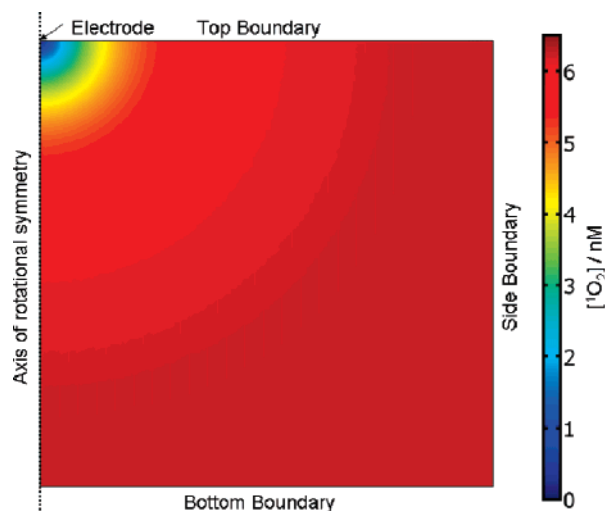

Figure 8. Numerical simulation of the singlet oxygen concentration profile in a perylene photosensitized system where oxygen is electrochemically reduced to the superoxide ion. The axis of rotational symmetry is perpendicular to the 7 μm disc ultramicroelectrode surface and runs through the center of the electrode. Singlet oxygen concentrations are defined using a color code. See the discussion in the text for the definition of the boundaries.

Table 2. Parameters Used in Simulating the Effects of Oxygen Reduction in CH₃CN

parameter	value
$\tau_{SO} = 1/(2k_d^{SO})$	2000 s
$\tau_{\Delta} = 1/k_d^{\Delta}$	80 μs[a]
k_q^{SO}	7×10^9 M^{-1} s^{-1} [b]
$D_O = D_{\Delta}$	7.1×10^{-5} cm^2 s^{-1} [c]
D_O/D_{SO}	2.8[d]
f_{Δ}^{S} [e]	0.27 ± 0.03[f]
f_{Δ}^{T}	1.00 ± 0.10[f]
f_{T}^{S}	0.68 ± 0.10[f]
f_T	~ 1[g]
Φ_T^0	0.03[f]
τ_S^a	6 ns[f]
k_q^{S}	3.8×10^{10} M^{-1} s^{-1} [f]

[a] From Scurlock and Ogilby.[26] [b] From Guiraud and Foote.[14] [c] From Tsushima et al.[27] [d] From Oshaka et al.[37] [e] Parameters relating to the sensitized production of singlet oxygen by perylene: f_{Δ}^{S} and f_{Δ}^{T} are the fractions of quenching events producing singlet oxygen from the sensitizer singlet and triplet states, respectively. The parameter f_{T}^{S} is the fraction of singlet quenching events yielding the sensitizer triplet state; f_T is the fraction of triplet states quenched by ground-state oxygen, Φ_T^0 is the triplet yield in the absence of oxygen, and k_q^{S} and τ_S are the rate constant for the oxygen quenching of and the lifetime of the sensitizer singlet state, respectively. [f] From Abdel-Shafi and Worrall.[32] [g] Estimated based on the triplet lifetime of perylene measured by Pirotta et al.[39]
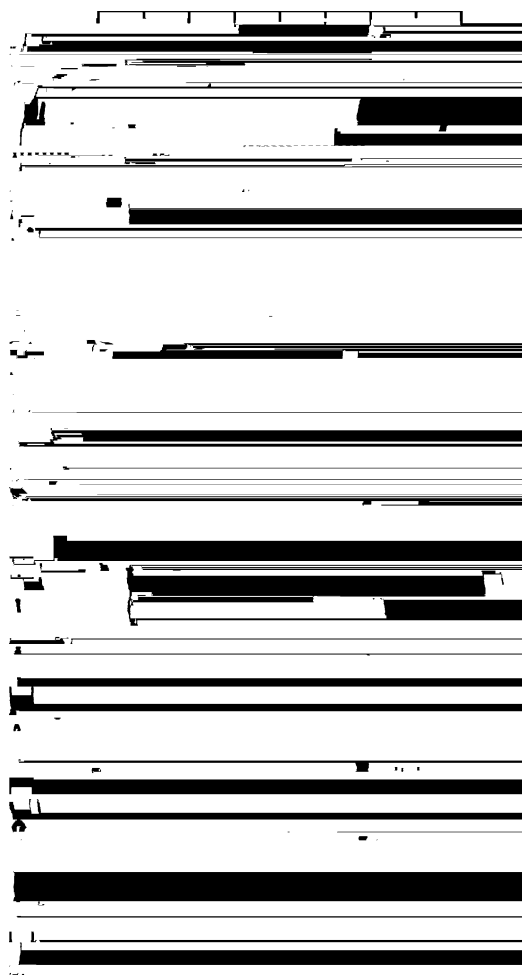

Figure 9. Simulated concentration profiles of the three oxygen-derived species in a dimension perpendicular to the electrode surface. (a) Ground-state oxygen and superoxide concentration are given on the left axis, and the singlet oxygen concentration on the right axis. The asymmetry between the ground-state oxygen and the superoxide profiles is due to the difference in diffusion coefficients of these two species. Singlet oxygen concentration profiles are modeled for two different cases: (1) excluding quenching of singlet oxygen by superoxide (dashed line) and (2) including quenching of singlet oxygen by superoxide (solid line). (b) Singlet oxygen concentration profiles using different superoxide lifetimes. The arrow indicates increasing superoxide lifetime (100, 500, 1000, 2000, and 5000 s).

respective molecules are slightly different.[38] All relevant parameters are collected in Table 2.

In Figure 8, we show the results of these simulations as a 2D plot of the singlet oxygen concentration. The hemispherical concentration profile around the electrode, as typically observed for ultramicroelectrodes, is apparent.[40] In examining the data, it is important to keep in mind that the singlet oxygen phosphorescence signal experimentally recorded using the singlet oxygen microscope is, in fact, a convolution of the singlet oxygen concentration profile modeled in Figure 8 with the microscope's point-spread function.[41] As a result, the experimental singlet oxygen phosphorescence profile contains a large component of

(37) Ohsaka, T.; Tsushima, M.; Okajima, T.; Tokuda, K. *Denki Kagaku* **1994**, *62*, 1300−1303.

(38) Poulsen, T. D.; Ogilby, P. R.; Mikkelsen, K. V. *J. Phys. Chem. A* **1998**, *102*, 8970−8973.

(39) Pirotta, M.; Renn, A.; Werts, M. H. V.; Wild, U. P. *Chem. Phys. Lett.* **1996**, *250*, 576−582.

(40) Bard, A. J. In *Scanning Electrochemical Microscopy*; Bard, A. J., Mirkin, M. V., Eds.; Marcel Dekker: New York, 2001.

(41) Shaw, P. J. In *Handbook of Biological Confocal Microscopy*, 2nd ed.; Pawley, J. B., Ed.; Plenum Press: New York and London, 1995; pp 373−385.

out-of-focus phosphorescence, yielding the observed poor contrast. In other words, the difference in experimental signal intensities for conditions of high and low oxygen concentration are not as pronounced as one might otherwise expect on the basis of the concentration profile modeled in Figure 8.

In Figure 9a, simulated concentration profiles for the three oxygen-derived species in a dimension perpendicular to the electrode surface are shown for a system using a 7 μm disc ultramicroelectrode. As a consequence of oxygen reduction to produce superoxide, the concentration of ground-state oxygen is completely depleted at the surface of the electrode but increases rapidly as the distance from the electrode increases. The concentration of oxygen limited by the ambient atmosphere is only reached at a distance of about 100 μm from the electrode. In turn, this leads to a lower yield of photosensitized singlet oxygen production in this 100 μm zone as seen from the singlet oxygen concentration profile. To specifically illustrate this latter point, the singlet oxygen profile was calculated in the absence of quenching by superoxide (dashed line in Figure 9a).

The simulations in Figure 9a also show that the concentration of superoxide near the electrode surface is very high, and that this concentration decreases as the distance from the electrode increases. Most importantly, however, there is an appreciable concentration of superoxide that extends several millimeters into the solution. When the quenching of singlet oxygen by superoxide is included in the simulation, the effect of this extensive superoxide distribution on the concentration profile of singlet oxygen is apparent. Specifically, the singlet oxygen concentration around the electrode is not only decreased, but the singlet oxygen concentration gradient now extends over a much larger zone around the electrode. These simulations suggest that quenching by superoxide is the main mechanism responsible for the reduction of the singlet oxygen phosphorescence signal observed around the electrode in Figure 6 and that the contribution from ground-state oxygen depletion due to the electrochemical reduction is minor. It should also be noticed that, as expected, the concentration profile of singlet oxygen is strongly dependent on the lifetime of superoxide (Figure 9b). Thus, the size of the singlet oxygen depletion zone around the electrode can also be manipulated by altering the superoxide lifetime (e.g., by changing solvent or adding trace amounts of water).

Conclusion

Using singlet oxygen microscopy, we have shown that concentrations of singlet oxygen produced in a photosensitized process can be both spatially and temporally controlled using an ultramicroelectrode. Two pathways to control were pursued: (1) local deactivation of the photosensitizer by oxidation or reduction, and (2) production of the singlet oxygen quencher, superoxide, by the reduction of oxygen. The photosensitizers examined (PD and Zn−TPP) all exhibited lower yields of singlet oxygen production upon application of a potential to the electrode, leading to a localized domain with a low concentration of singlet oxygen. As the electrode potential was turned off, the unreduced or unoxidized photosensitizer populations were regained leading to a total recovery of the singlet oxygen population. Experiments are currently being performed to identify a sensitizer system that exhibits the inverse behavior, thus allowing one to switch the sensitizer on by applying a potential. For sensitizers with reduction potentials more negative than that for the reduction of ground-state oxygen to superoxide, quenching of singlet oxygen by superoxide was observed, again leading to a singlet oxygen depletion zone. On the basis of numerical simulations, the role of ground-state oxygen depletion due to the electrochemical reduction was estimated to be insignificant in this process. Singlet oxygen removal caused by superoxide quenching was likewise found to be reversible, as the singlet oxygen signal could be recovered upon reoxidizing superoxide at the electrode surface. The size of the depletion zone caused by superoxide quenching could be controlled by adjusting the applied potential. Furthermore, simulations showed that the zone could also be manipulated by changing the superoxide lifetime. Depending on the applied potential, the effects of superoxide quenching and sensitizer redox chemistry can be used additively or separately.

In conclusion, one can indeed use electrochemical manipulations to affect spatial and temporal control of singlet oxygen populations in a photosensitized experiment. Future work will address the extent to which this methodology can be used in controlling populations of singlet oxygen in aqueous solutions and eventually in heterogeneous and biologically relevant systems.